ACS APPLIED MATERIALS & INTERFACES

Research Article

www.acsami.org

Porphyrin-Sensitized Solar Cells: Effect of Carboxyl Anchor Group Orientation on the Cell Performance

Aaron S. Hart, Chandra B. KC, Habtom B. Gobeze, Lindsey R. Sequeira, and Francis D'Souza*

Department of Chemistry, University of North Texas, 1155 Union Circle, #305070, Denton, Texas 76203-5017, United States

Supporting Information

ABSTRACT: The effect of the orientation of the porphyrin sensitizer onto the TiO_2 surface on the performance of dye-sensitized solar cells (DSSCs) is reported. Free-base and zinc porphyrins bearing a carboxyl anchoring group at the para, meta, or ortho positions of one of the *meso*-phenyl rings were synthesized for application in Grätzel-type photoelectrochemical cells. The remainder of the *meso*-phenyl rings was substituted with alkyl chains of different length to visualize any aggregation effects. Absorption and fluorescence studies were performed to characterize and observe spectral coverage of the thirteen newly synthesized porphyrin derivatives. Photoelectrochemical studies were performed after immobilization of porphyrins onto nanocrystalline TiO_2 and compared with DSSC constructed using N719 dye as reference. The performance of DSSCs with the porphyrin anchoring at the para or meta position were found to greatly exceed those with the anchoring group in the ortho position. Additionally, cells constructed using zinc porphyrin derivatives outperformed the free-base porphyrin analogs. Better dye regeneration efficiency for the zinc porphyrin derivatives compared to their free-base porphyrin analogs, and for the meta and para derivatives over the ortho derivatives was evaluated from electrochemical impedance spectroscopy studies. Femtosecond transient absorption spectroscopy studies were performed to probe the kinetics of charge injection and charge recombination with respect to the orientation of porphyrin macrocycle on TiO_2 surface. The ortho porphyrin derivative with an almost flat orientation to the TiO_2 surface revealed fast charge recombination and suggested occurrence of through-space charge transfer. The overall structure-performance trends observed for the present porphyrin DSSCs have been rationalized based on spectral, electrochemical, electrochemical impedance spectroscopy, and transient spectroscopy results.

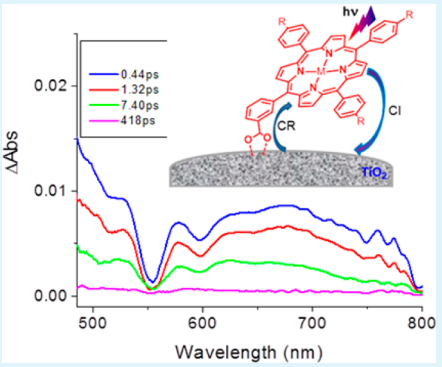

KEYWORDS: *photoelectrochemistry, porphyrin, dye orientation, organic solar cell, impedance spectroscopy, light energy conversion, femtosecond transient spectroscopy*

1. INTRODUCTION

Dye-sensitized solar cells (DSSCs), often known as Grätzel cells, have garnered significant attention as promising low-cost alternatives to expensive Si-based solar cell technology.[1−12] In typical DSSCs, mesoporous titanium dioxide (TiO_2) decorated with photosensitizer dye molecules inject electrons into the conduction band of TiO_2 in contact with an electrolyte solution, achieving light into electricity conversion.[13−41] Organic photosensitizers capable of wide spectral capture are considered to be cheaper alternatives for DSSC applications, potentially replacing the originally designed, rather expensive ruthenium-based metal complex sensitizers. Additionally, organic dyes possess higher extinction coefficients, leading to greater light harvesting abilities. Common solar dye design involves an electron donor photosensitizer connected to an electron acceptor that doubles as an anchoring functional group. Coumarins, quantum dots, triphenylamines, phenothiazine, phthalocyanine, and porphyrin are commonly implemented as photosensitizers.[42−108]

Among the different organic dyes, functionalized porphyrins are frequently used sensitizers.[84−108] These tetrapyrrole macrocycles, in their free-base form or with a redox inactive metal such as zinc inside the macrocycle cavity, reveal strong light absorption with a Soret band in the 400−450 nm range and visible bands in the 500−650 nm range. In fact, the highest efficiency solar cell reported to-date (η = 12.3%) is of a zinc porphyrin-based dye molecule.[108] One key issue to consider in designing porphyrin dyes relates to the position of the anchoring group in relation to the plane of macrocycle π-system. In a majority of the porphyrin-derived dyes, the carboxyl anchoring group was positioned in such a way that the porphyrin was orthogonal to the TiO_2 surface, although few studies have shown that the positioning of carboxyl group vary the performance of the solar cells.[100−104]

In the present study, thirteen porphyrin derivatives, six free-base and seven zinc-metalated, are investigated by varying the position of the carboxyl anchoring group: para (**1p**, **1p-Zn**, **2p**, **2p-Zn**, **3p-Zn**), meta (**1m**, **1m-Zn**, **2m**, **2m-Zn**, **3m**, **3m-Zn**), and ortho (**1o** and **1o-Zn**), and length of the alkyl substituents on the remaining three phenyl rings for their cell performance (see Figure 1 for structures). As shown in Figure 2, as a result of fairly

Received: April 2, 2013
Accepted: May 6, 2013
Published: May 6, 2013

   dx.doi.org/10.1021/am401201q | ACS Appl. Mater. Interfaces 2013, 5, 5314−5323

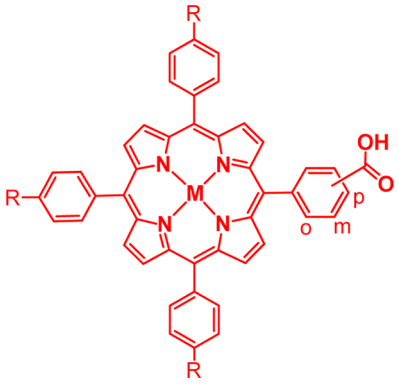

R = -CH_3; M = 2H; para **1p**
R = -CH_3; M = 2H; meta **1m**
R = -CH_3; M = 2H; ortho **1o**
R = -CH_3; M = Zn; para **1p-Zn**
R = -CH_3; M = Zn; meta **1m-Zn**
R = -CH_3; M = Zn; ortho **1o-Zn**
R = -$(OCH_2CH_2)_3OCH_3$; M = 2H, para **2p**
R = -$(OCH_2CH_2)_3OCH_3$; M = 2H, meta **2m**
R = -$(OCH_2CH_2)_3OCH_3$; M = Zn, para **2p-Zn**
R = -$(OCH_2CH_2)_3OCH_3$; M = Zn, meta **2m-Zn**
R = -$CH_2CH_2CH_3$; M = 2H, meta **3m**
R = -$CH_2CH_2CH_3$; M = Zn, para **3p-Zn**
R = -$CH_2CH_2CH_3$; M = Zn, meta **3m-Zn**

Figure 1. Structures of the synthesized porphyrin derivatives with the anchoring carboxyl group located either at the para, meta, or ortho position of one of the phenyl rings.

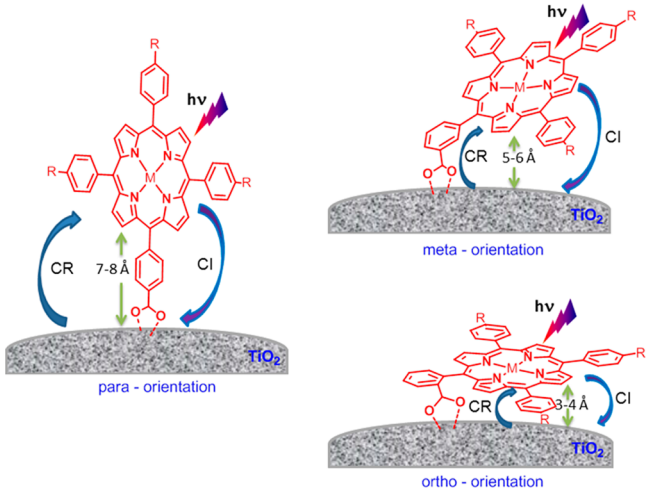

Figure 2. Relative orientation of para, meta, and ortho carboxyphenyl functionalized porphyrin adsorbed on TiO_2 surface. Key photochemical events responsible for cell performance are also shown (CI, charge injection; CR, charge recombination).

rigid bidentate type binding of the carboxyl group on TiO_2,[100−104] the para derivatives would largely position the porphyrin π-system orthogonal to the TiO_2 surface; meta derivatives would position the π-system at an angle (50−80°), which could favor both through-bond and through-space interactions; and the ortho derivatives would bring the π-system even closer to the TiO_2 surface facilitating stronger through-space interactions between them. Thus a minor modification of carboxyl functionality would change the relative orientation of the porphyrin with respect to TiO_2 surface, and would contribute to the overall cell performance. We report these findings from a systematic study performed using different techniques.

2. RESULTS

The syntheses of the free-base porphyrin derivatives was carried out according to the traditional Adler-Longo method by reacting stoichiometric amounts of pyrrole and functionalized benzaldehydes in propionic acid followed by chromatographic separation over silica gel.[109] The free-base porphyrins were metalated using zinc acetate in refluxing chloroform/methanol solution while monitoring the completeness of the reaction by recording the disappearance of the 515 nm band of the free-base porphyrin.[110] The purity of all the porphyrin derivatives was checked on thin-layer chromatography prior to performing any studies.

Optical Absorbance and Steady-State Fluorescence Studies. The optical absorption and emission spectra of the carboxyl functionalized porphyrins in chloroform/methanol mixture were not significantly different from their parent derivatives, viz., tetrakis(4-alkylphenyl)porphyrins.[111,112] Representative absorption and emission spectrum of **1p-Zn** is shown in Figure 3. The free-base porphyrins exhibited a strong Soret in the

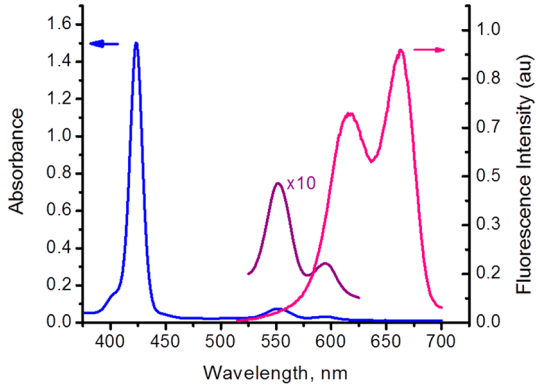

Figure 3. Absorption and fluorescence spectrum of **1p-Zn** in chloroform−methanol mixture. The Q-band region is magnified for clarity.

420 nm range and four visible bands in the 500−675 nm range while for zinc porphyrins the Soret was red-shifted by about 5 nm compared to the respective free-base porphyrin analog and two visible bands in the 525−575 nm range, due to increased symmetry, were observed. The fluorescence spectra of the free-base porphyrins revealed strong emission around 650 with a shoulder band at 720 nm, whereas for the zinc porphyrins, these emission bands were at 615 and 665 nm, respectively.

The expected two one-electron oxidation and two one-electron reduction for each of the porphyrin derivatives were also observed.[113] The zinc porphyrin derivatives were easier to oxidize by about 220 mV compared to their free-base porphyrin analogs (Figure 4). Further, to visualize the spectral features of the oxidized electron donor sensitizer porphyrin, compounds **1p-Zn**, **1m-Zn**, and **1o-Zn** were chemically oxidized by the addition of one equivalent of nitrosonium tetrafluoroborate in methanol. Figure 5 shows spectral changes for **1p-Zn** whereas for **1m-Zn** and **1o-Zn**, the spectral are shown in the Supporting Information. New bands with peak maxima at 660 nm and at 845 nm were apparent for the ZnP^{+} species.

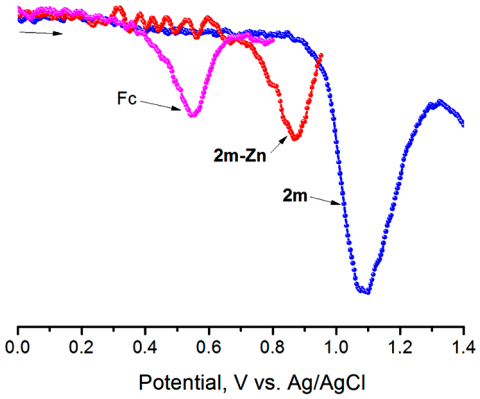

Figure 4. Differential pulse voltammograms showing first oxidations of **2m**, **2m-Zn**, and ferrocene (used as internal standard) in DMF containing 0.1 M $(TBA)ClO_4$.

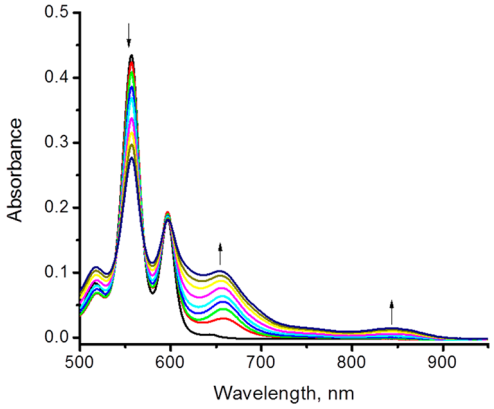

Figure 5. Chemical oxidation of porphyrin **1p-Zn** using nitrosonium tetrafluoroborate (0.15 eq. each addition) in methanol.

Photoelectrochemical Studies. Figure 6 shows the $J-V$ characteristics of DSSC employing each of the porphyrin derivatives as photosensitizers under AM1.5 solar illumination conditions. Both working and counter electrodes were sandwiched together, using the thin film TiO_2 as the working electrode and Pt-ized FTO as the counter electrode and employing a solution containing I^-/I_3^- as the redox mediator between the electrode interfaces. To avoid dye aggregation, the electrodes were soaked for 4 h in 0.2 mM dye solution. Losses due to light reflection from the surface of the electrodes have not been corrected. On−off switching experiments were performed, resulting in steady photocurrent in the reported electrodes. The open-circuit potential (V_{oc}), short-circuit current (J_{sc}), fill factor (FF), and quantum efficiency (η) for each photosensitizer[114] are reported in Table 1. The highest efficiency obtained for the free-base porphyrins was 0.72%, using porphyrin **1m**, which employed both a tolyl substituent and an anchoring group at the meta position with respect to the macrocycle. After zinc metalation, the cell under the same experimental conditions showed an increased efficiency, that is, 3.13% for **1p-Zn** and 4.17% for **1m-Zn** were observed. The performance of **1p-Zn** under the present experimental conditions was slightly lower than that reported earlier by Imahari et al.[89] In either case, both porphyrins showed an increased efficiency over porphyrins with an ortho-carboxylic acid group, porphyrins **1o** and **1o-Zn**. The same trend was seen with the para porphyrins with the same substituents (**1p** and **1p-Zn**). When comparing para and meta derivatized porphyrins, neither seemed to exceed the other when focusing on the same R-groups. Porphyrins bearing propyl chains and ethylene glycol chains in both para (**2p, 2p-Zn, 3p-Zn**) and meta (**3m, 3m-Zn 2m, 2m-Zn**) cases showed to be indifferent,

Table 1. Photovoltaic Performance[a] of DSSCs based on the Synthesized Porphyrin Derivative Dyes with Liquid Electrolyte

dye	J_{sc} (mA/cm^2)	V_{oc} (V)	FF	η (%)	amount (mol/cm^2)
N719	18.13	0.62	0.66	7.39	
1p	1.26	0.45	0.75	0.42	
1p-Zn	6.67	0.59	0.79	3.13	1.76×10^{-7}
1m	2.06	0.48	0.72	0.71	
1m-Zn	8.42	0.65	0.82	4.17	2.19×10^{-7}
1o	0.31	0.45	0.83	0.11	
1o-Zn	1.01	0.51	0.71	0.37	1.32×10^{-7}
2p	1.17	0.52	0.82	0.65	
2p-Zn	4.82	0.60	0.77	2.42	
2m	1.61	0.55	0.74	0.65	
2m-Zn	5.19	0.61	0.78	2.45	
3p-Zn	4.88	0.57	0.76	2.09	
3m	0.78	0.52	0.74	0.30	
3m-Zn	3.01	0.56	0.73	1.99	

[a]Average of three DSSCs.

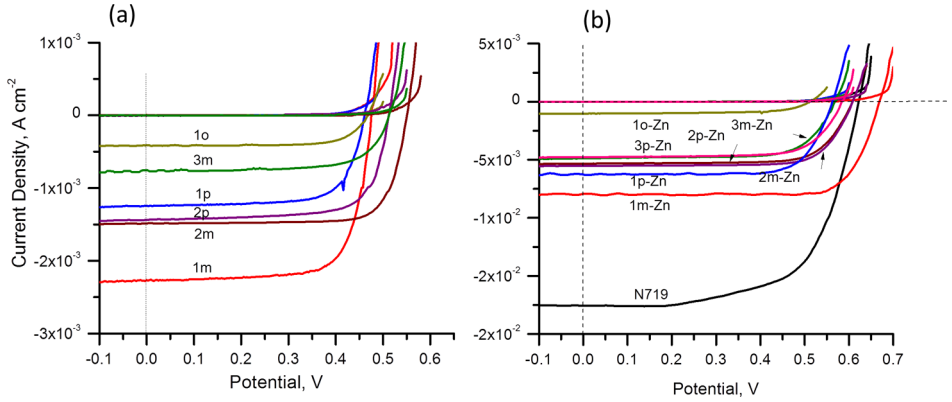

Figure 6. Photocurrent density vs voltage ($J-V$) curves of DSSCs built using (a) free-base porphyrin derivatives, and (b) zinc metalated porphyrin derivative as sensitizers under irradiation of AM 1.5G simulated solar light (100 mW cm^{-2}) in the presence of I^-/I_3^- redox mediator (0.6 M propyl methyl iodide (PMII), 0.1 M LiI, 0.05 M I_2, and 0.5 M *ter*-butyl pyridine (TBP)) in acetonitrile.

dx.doi.org/10.1021/am401201q | ACS Appl. Mater. Interfaces 2013, 5, 5314−5323

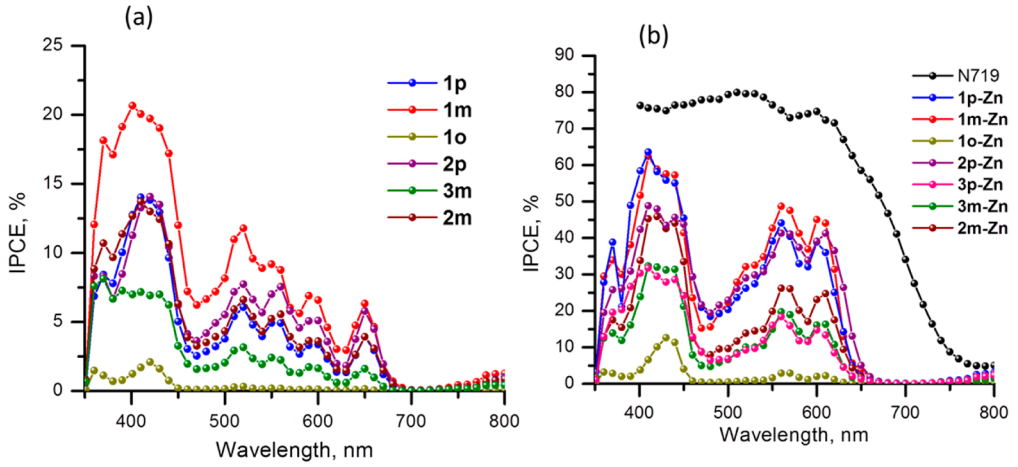

Figure 7. Incident photon-to-current conversion action (IPCE %) spectra of mesoporous TiO_2 electrodes sensitized with (a) free-base and (b) zinc metalated porphyrins in acetonitrile containing I^-/I_3^- (0.6 M propyl methyl iodide (PMII), 0.1 M LiI 0.05 M I_2, and 0.5 M *ter*-butyl pyridine (TBP)) redox mediator using an AM 1.5 simulated light source with a 350 nm UV-cut off filter.

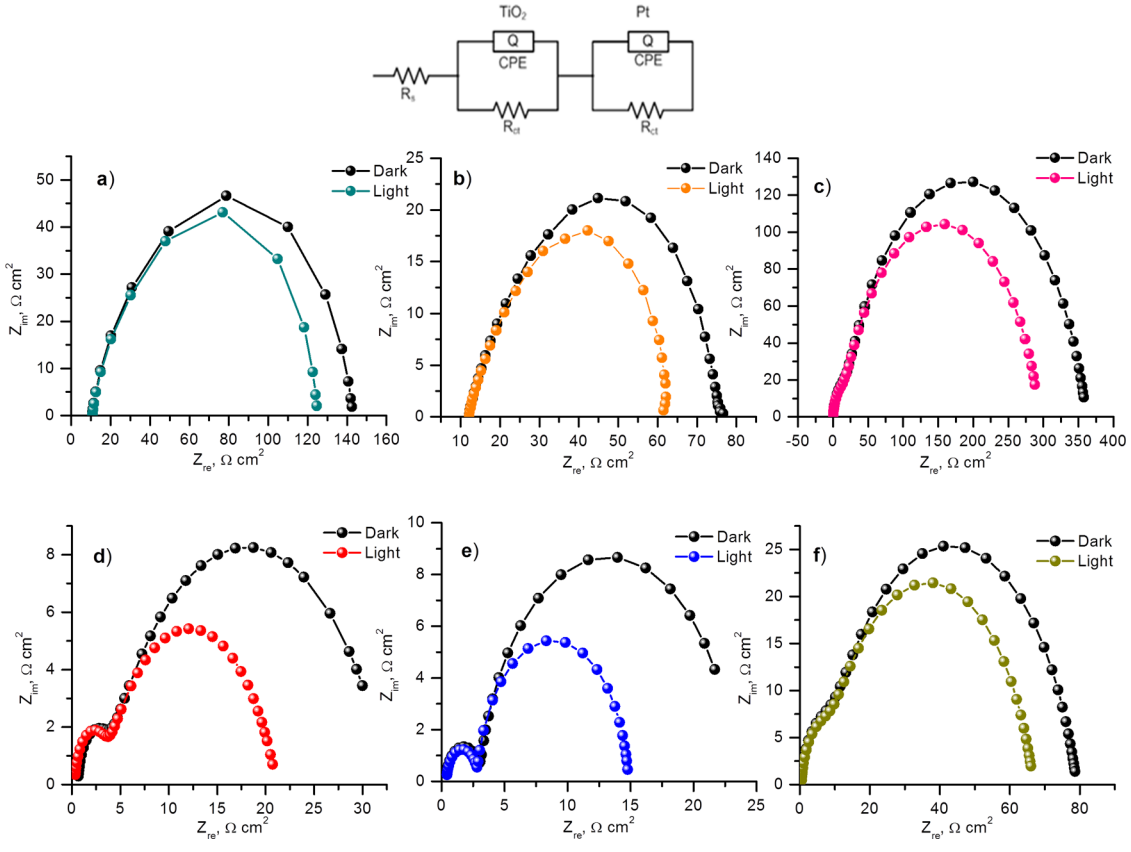

Figure 8. Nyquist plots for (a) FTO/TiO_2/**1p**, (b) FTO/TiO_2/**1m**, (c) FTO/TiO_2/**1o**, (d) FTO/TiO_2/**1p-Zn**, (e) FTO/TiO_2/**1m-Zn**, and (f) FTO/TiO_2/**1o-Zn** measured at respective V_{oc} under dark (black line) and AM 1.5 filtered light illumination (colored line) conditions. The figure shown at the top is of the equivalent circuit diagram used to extract the parameters.

suggesting that either orientation is optimal for cell performance. The data in Table 1 also suggest that the better performance of the zinc over free-base porphyrin derivatives is due to not only increased J_{sc} but also increased V_{oc} and to some extent better fill-factor.

The incident photon-to-current conversion efficiency (IPCE), defined as the number of electrons generated by the light in the outer circuit divided by the number of incident photons, as given by eq 1:[115]

$$\mathrm{IPCE}(\%) = 100 \cdot 1240 I_{SC}(\mathrm{mA\ cm^{-2}}) / [\lambda(\mathrm{nm}) P_{in}(\mathrm{mW\ cm^{-2}})] \quad (1)$$

where I_{sc} is the short-circuit current generated by incident monochromatic light illumination and λ is the wavelength of this light at an intensity of P_{in}. The IPCE spectra are shown in Figure 7.

In general, all porphyrins generated appreciable amounts of photocurrent over the range of 350−650 nm for zinc and 350−

dx.doi.org/10.1021/am401201q | ACS Appl. Mater. Interfaces 2013, 5, 5314−5323

700 nm range for free-base porphyrins. IPCE performance of N719 DSSC has also been included for reference. Porphyrin **1m-Zn** showed the greatest photocurrent over the region of 500−650 nm, supporting the improved quantum efficiency. Porphyrin **1p-Zn** showed similar IPCE values for the Soret band, but reduced values for the Q bands. As expected, porphyrins **1o** and **1o-Zn** exhibited the lowest IPCE values of the entire group, in agreement with the decreased η values.

The amount of porphyrin adsorbed was calculated by desorbing the adsorbed porphyrin on the TiO_2 surface by the addition of hydroxide for electrodes made out of porphyrins **1p-Zn**, **1m-Zn**, and **1o-Zn**. As shown in Table 1, the amount of adsorbed dye was slightly higher for **1p-Zn** and **1m-Zn** compared to **1o-Zn**, although all of them were soaked in porphyrin solutions of same concentration (0.2 mM) and same period of time (4 h). These observations suggest that the flat orientation of adsorbed porphyrin with respect to the TiO_2 surface of the ortho derivative (see Figure 2) results in slightly less dye intake compared to the meta and para derivatives.

Electrochemical Impedance Spectroscopy Studies. Electrochemical impedance spectroscopy (EIS) studies were performed as this tool is known to be useful in estimating electron recombination resistance and observing the dye regeneration efficiency.[116,117] The Nyquist plots of the free-base porphyrin (Figure 8a−c) and zinc porphyrin (Figure 8d−f) show two semicircles, where the smaller semicircles in high frequency range reflect the charge transfer at the counter electrode/electrolyte interface. The larger semicircles in the low-frequency range correspond to the TiO_2/porphyrin/redox (I^-/I_3^-) electrolyte interface. After analyzing the curves using an equivalent circuit (Figure 8 top), the charge transfer resistance of the counter electrode/electrolyte interface, R_{CT}(Pt) were found to be small under both light illumination and dark conditions (Table 2). Interestingly, substantially lower charge transfer resistance was obtained for the TiO_2/porphyrin/redox interface, R_{CT}(Pt) under light illumination compared to the value gathered in dark conditions.

Table 2. Charge Transfer Resistance Values of FTO/TiO_2/Porphyrin and Counter Pt Electrodes (at the respective V_{oc}) Estimated Using Electrochemical Impedance Spectroscopy

	$R_{CT}(TiO_2)$ (Ω cm^2)		R_{CT}(Pt) (Ω cm^2)	
dye	dark	light	dark	light
1p	126.9	109.0	11.9	15.5
1p-Zn	29.5	17.8	2.7	3.0
1m	54.1	38.2	5.8	7.7
1m-Zn	20.5	12.0	2.6	2.4
1o	346.9	281.0	14.3	13.4
1o-Zn	71.5	59.2	7.3	7.2

Additional observations with respect to the metal ion in the porphyrin cavity and the position of carboxyl group substitution were also made. Generally, a decrease in $R_{ct}(TiO_2)$ can be attributed to superior photoregeneration ability which would support an increased efficiency of the solar cells. The observed trend in $R_{ct}(TiO_2)$ for a given series was meta < para < ortho, and zinc porphyrin < free-base porphyrin. The FTO/TiO_2/**1o** showed the greatest charge transfer resistance of 346.9 and 281.0 Ω cm^2, under dark and light conditions, respectively. Zinc metalation improved these values to 71.5 and 59.2 Ω cm^2 under dark and light conditions, respectively; however, these values were much higher compared to FTO/TiO_2/**1p-Zn** and FTO/TiO_2/**1m-Zn**. That is, FTO/TiO_2/**1p-Zn** exhibited $R_{ct}(TiO_2)$ values of 29.5 Ω cm^2 under dark conditions and 17.8 Ω cm^2 under AM 1.5 filtered light illumination, whereas FTO/TiO_2/**1m-Zn** showed reduced R_{ct} values of 20.5 and 12.0 Ω cm^2, under dark and light conditions, respectively. A similar trend was also observed for the free-base porphyrin derivatives (see data in Table 1). These results support the overall lower efficiency of the ortho porphyrin derivatives compared to either of meta or para derivatives.

Femtosecond Transient Absorption Spectral Studies. In the present study, we have also made an effort to seek a correlation between the orientationof the dye on TiO_2 surface and electron transfer dynamics of the porphyrin modified FTO/TiO_2 electrodes. Zinc porphyrins **1p-Zn**, **1m-Zn**, and **1o-Zn**, representing para, meta, and ortho derivatives, were employed as they provided the highest energy conversion efficiencies. First, the porphyrins were characterized in solution to get properties of the involved excited states and optimize the spectral region to probe interfacial electron transfer process.

Figure 9 shows transient absorption spectra of **1p-Zn** and **1m-Zn** in *o*-dichlorobenzene solution measured at several time intervals after excitation at 400 nm at the Soret region (see the Supporting Information for **1o-Zn**). In agreement with the literature results on femtosecond transient spectra of carboxyl functionalized zinc porphyrin derivatives,[118,119] excitation using 400 nm laser light instantly populated (<2 ps) the S_2 state of zinc porphyrin with maximum at ∼480 nm. At higher wavelength region, two depleted signals at 550 and 588 nm, opposite mimic of the ground state absorption of the Q-bands in Figure 3, were observed. With time, the 588 nm band revealed small red-shift and appeared at 594 nm in the region of Q(0,0) band of steady state emission. The Q(0,1) emission band was also observed at ∼668 nm. Collectively, these results point out the occurrence of depleted absorption of the S_0 to S_1 transition and stimulated emission of the S_1 to S_0 state in the transient absorption spectra within the monitored time and spectral window.

Electron injection from surface adsorbed zinc porphyrin to semiconductive TiO_2 would result in the generation of oxidized zinc porphyrin, $ZnP^{\cdot+}$ and reduced TiO_2. Chemical oxidation of compounds **1p-Zn**, **1m-Zn**, and **1o-Zn** revealed a relatively strong band at 660 nm and a weaker band at 840 nm as shown in Figure 5. Thus, observation of these bands would serve as a diagnostic indication for charge injection, and their rise and decay would provide quantitative information of the kinetics of charge injection and charge recombination. Panels a and c in Figure 10 show transient spectra of FTO/TiO_2/**1m-Zn** and FTO/TiO_2/**1o-Zn** electrodes at different delay times (see the Supporting Information for FTO/TiO_2/**1p-Zn** spectra). Distinct spectral features from that observed for the pristine zinc porphyrin probe in Figure 9 were observed. A broad band in the 600−700 nm region characteristic of $ZnP^{\cdot+}$ was observed that tracked the S_2 and S_1 states of zinc porphyrin, suggesting both these states are involved in charge injection.

Panels b and d in Figure 10 show the time profile of the absorption changes at 660 nm band. The rise was completed within 0.37−0.42 ps for all three porphyrin derivatives suggesting ultrafast charge injection. Interestingly, the decay representing the charge recombination lasted for 60−90 ps depending upon the porphyrin isomer and could be fitted to three-exponential fit as shown in Table 3. Although for the first two fast decay components it was difficult to see a trend, for the slow decaying component, a clear trend was observed. That is, the charge recombination was much faster for **1o-Zn** compared to **1p-Zn** or

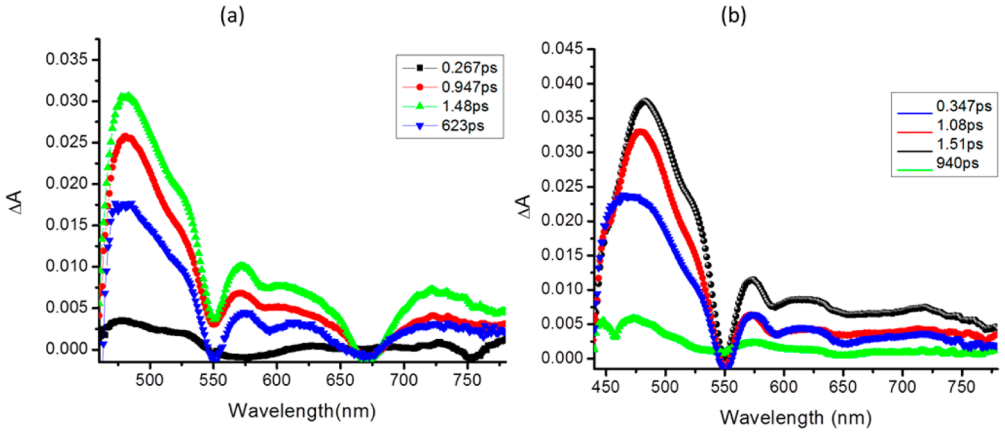

Figure 9. Femtosecond transient absorption spectra of (a) **1m-Zn** and (b) **1p-Zn** in *o*-dichlorobenzene at the indicated delay times. The samples were excited with 400 nm femtosecond (100 fs) laser pulses.

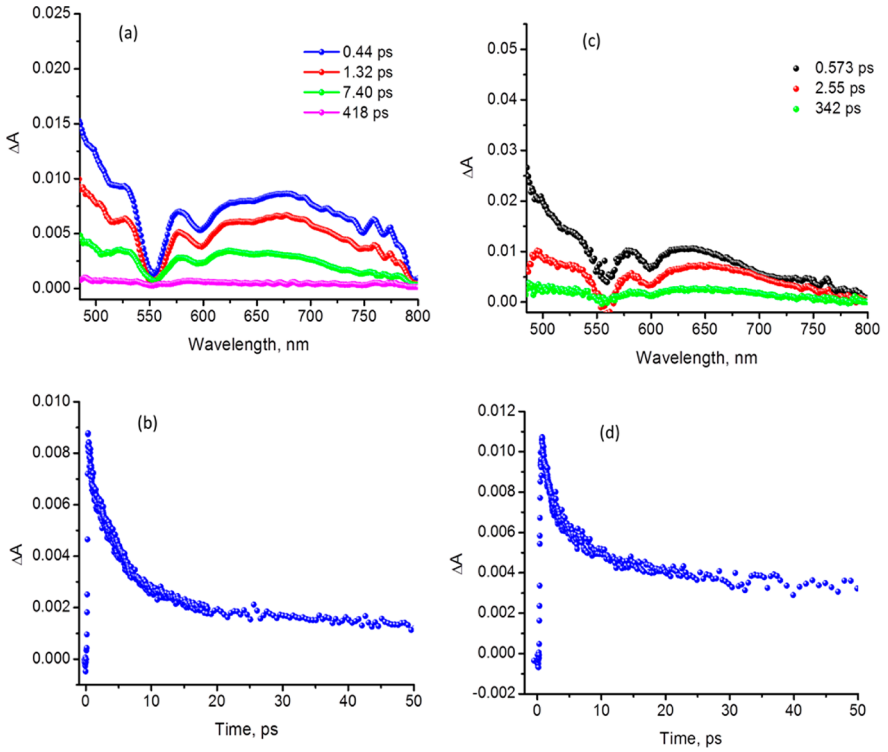

Figure 10. Femtosecond transient absorption spectra of (a) FTO/TiO_2/**1m-Zn** and (c) FTO/TiO_2/**1o-Zn** electrodes at the indicated delay times. The samples were excited using 400 nm laser pulses of 100 fs. The time profile of the 660 nm band corresponding to $ZnP^{\bullet+}$ is shown in panels b and d, respectively, for FTO/TiO_2/**1m-Zn** and FTO/TiO_2/**1o-Zn**.

Table 3. Kinetics of Charge Injection and Charge Recobmination of FTO/TiO_2:Zinc Porphyrin Electrodes

electrode	rise τ_{av} (ps)	decay τ_1 (ps)[a]	decay τ_2 (ps)[a]	decay τ_3 (ps)[a]
FTO/TiO_2:**1p-Zn**	0.30	1.5 (51.2%)	17.8 (21.4%)	88.6 (27.4%)
FTO/TiO_2:**1m-Zn**	0.42	3.5 (59.1%)	10.3 (21.9%)	66.2 (19.0%)
FTO/TiO_2:**1o-Zn**	0.37	1.6 (52.2%)	15.7 (33.1%)	62.7 (14.7%)

[a]Values in paratheses show percent pre-exponential values.

1m-Zn modified electrodes, perhaps being oriented parallel to the TiO_2 surface.[93]

3. DISCUSSION

Several interesting observations could be made from the present study that used a relatively simple series of free-base and zinc metalated tetraarylporphyrin derivatives functionalized with a carboxyl group at the para, meta, or ortho positions of one of the meso-phenyl substituents. The free-base porphyrin derivatives had better spectral coverage in the Q-band region compared to the zinc porphyrin analogs. However, they differed in their oxidation potentials, that is, the zinc porphyrins were easier to oxidize by about 220 mV compared to free-base porphyrins. It is generally accepted that the carboxyl group binds to the TiO_2 surface as a bidentate ligand using both oxygens.[100−104] This leads to a relatively rigid orientation with respect to the reasonably large suface of TiO_2 (20 nm;18 NRT, Dyesol).

dx.doi.org/10.1021/am401201q | *ACS Appl. Mater. Interfaces* 2013, 5, 5314−5323

Consequently, although fairly close to the surface in all three cases, the estimated macrocycle edge-to-edge distance to the surface of TiO_2 varied as para (7−8 Å) > meta (5−6 Å) > ortho (3−4 Å) (see Figure 2). The alkyl groups on the three aryl rings were also varied to a short methyl group to a medium propyl group to the longer triethyleneoxide groups. Although these groups did not significantly purturb either the spectral or redox properties of the porphyrin macrocycle, the long alkyl chains improved the solubility and were expected to reduce the aggregation of porphyrin when immobilized on the TiO_2 surface.

The photoelectrochemical $J-V$ plots and IPCE curves revealed the anticipated structure-performance properties. For a given type of porphyrin (para, meta, or ortho carboxyl substituent), irrespective of the nature of the alkyl groups, the zinc porphyrins outperformed the free-base porphyrins. Reduced V_{oc} and J_{sc} of free-base porphyrin derived photocells contributed to this cause. The IPCE curves in Figure 7 revealed the expected better spectral coverage (350−700 nm) for the free-base porphyrin derived cells compared to zinc porphyrin (300−650 nm) derived cells, however, the former revealed lower IPCE values. In fact, the maximum IPCE observed for **1m** at the Soret region was 23% which compared with a value of 64% for the zinc porphyrin derivative, **1m-Zn**. The easier to oxidize zinc porphyrin derivatives seem to have a better performance although they revealed less spectral coverage. The presence of long-alkyl chains on porphyrin macrocycle did not necessarily help improve the performance of the photocells, indeed, the best results were obtained for cells made out of tolyl substituents. This observation suggests that by lowering the dye-adsorption time, one could avoid dye aggregation that would reduce the cell performance. For a given series of para, meta, or ortho porphyrin derivaties, the para and meta derivatives outperformed cells constructed using ortho derivatives. It may be mentioned here that the density of the adsorbed dye for the ortho porphyrin derivative was slightly lower than the other two (see Table 1), although this fact alone could not explain its lower efficiency.

The electrochemical impedance spectroscopic studies of estimation of charge transfer resistance, R_{CT} related to photoregeneration efficiency of the employed porphyrin sensitizers, and femtosecond transient absorption spectral studies to evaluate kinetics of charge injection and charge recombination from the singlet excited porphyrin to TiO_2 in FTO/TiO_2/porphyrin were useful to further understand the performance of the investigated solar cells. The R_{CT} (TiO_2) values were larger for a given free-base porphyrin compared to its zinc porphyrin analog, in some case by an order of magnitude. Additionally, the para and meta derivatives revealed the lowest R_{CT} (TiO_2) over the ortho derivatives. It has been possible to spectrally characterize the one-electron oxidized product of zinc porphyrin in the wavelength region of 660 nm by femtosecond transient spectroscopic technique. Ultrafast charge injection from singlet excited zinc porphyrin to TiO_2 with a time constant less than 0.42 ps was observed for FTO/TiO_2/zinc porphyrin electrodes. Interestingly, the faster charge recombination in the cases of ortho derivative was apparent. This also brings out another important aspect of through-bond and through-space charge transfer.[93] Because all of the derivatives have similar carboxyl linker, any variations in the rates mean contributions from through-space electron transfer in addition to any through-bond contributions. The fast charge recombination in the case of the ortho derivative where the porphyrin macrocycle is much closer to the TiO_2 surface, followed by the meta and para, is supportive of through-space electron transfer events.

4. SUMMARY

In summary, thirteen porphyrin dyes functionalized with a carboxylic acid anchoring group at the para, meta, or ortho positions of one of the phenyl rings of meso-tetra aryl porphyrin in addition to varying functional groups of the remaining meso positions of the porphyrin ring, were newly synthesized to probe the effect of dye-orientation on TiO_2 surface on their photoelectrochemical performance. Porphyrins were successfully absorbed onto thin film TiO_2 on FTO and utilized in building DSSCs of two-electrode assembly. The absorption and emission, as well as electrochemical properties were studied to evaluate spectral coverage of free-base and zinc porphyrins as well as their excited state oxidation potentials. It was found that porphyrins anchored to the mesoporous TiO_2 in the para and meta positions with respect to the porphyrin ring were found to have improved photoelectrochemical properties compared to their ortho counterparts. This was supported by femtosecond transient absorption spectroscopy data collected on zinc−metalated porphyrin derivatives, showing fast charge recombination time for the ortho derivative adsorbed electrode. Similarly, placing tolyl groups in the three remaining meso positions showed improved efficiency compared to the long alkyl chain and ethylene oxide groups mentioned in this study. Additionally, the zinc porphyrin derivatives outperformed their free-base porphyrin counterparts. These data are supported by R_{CT} (TiO_2) values, determined from electrochemical impedance spectral studies, being less for those with zinc at the center of macrocycle cavity. The time-resolved transient absorption studies were also suggestive of occurrence of through-space electron transfer as against through-bond processes.

5. EXPERIMENTAL SECTION

Chemicals. All of the reagents were from Aldrich Chemicals (Milwaukee, WI), whereas the bulk solvents utilized in the syntheses were from Fischer Chemicals.

Syntheses of Free-Base Porphyrins.[109] In a typical synthesis, 10 mmol of 4-alkyl substituted benzaldehyde, 3.33 mmol of (*o*, *m*, or *p*)-formylbenzoic acid and 13.32 mmol of pyrrole were refluxed for 5 h in 150 mL of propionic acid. After cooling the mixture at room temperature, the solvent was evaporated and the dark black colored crude compound was purified by silica gel column. All the desired compounds were eluted by $CHCl_3$:MeOH (90:10 v/v) and the purity was checked by thin-layer chromatography.

*5-(4-Carboxyphenyl)-10,15,20-tris(tolyl)porphyrin, (**1p**)-*. Yield: 12%. ^{1}H NMR ($CDCl_3$: 400 MHz), δ ppm: −2.45 (s, 2H, −NH), 2.75 (s, 9H, $-CH_3$), 7.55 (d, 6H, phenyl H), 8.10 (dd, 6H, phenyl H), 8.30 (d, 2H, phenyl H), 8.45 (d, 2H, phenyl H), 8.82 (d, 2H, pyrrole), 8.92 (m, 6H, pyrrole H).

*5-(3-Carboxyphenyl)-10,15,20-tris(tolyl)porphyrin (**1m**)*. Yield: 12.5%. ^{1}H NMR ($CDCl_3$:400 MHz), δ ppm: −2.81 (s, 2H, −NH), 2.70 (s, 9H, $-3CH_3$), 7.59 (d, 6H, phenyl H), 7.85 (m, 2H, phenyl H), 8.10 ppm (d, 6H, phenyl H), 8.40 (d, 1H, phenyl H), 8.50 (d, 1H, phenyl H), 8.80 (m, 2H, pyrrole H), 8.90 (m, 6H, pyrrole H).

*5-(2-Carboxyphenyl)-10,15,20-tris(tolyl)porphyrin (**1o**)*. Yield: 10.5%. ^{1}H NMR ($CDCl_3$:400 MHz) δ ppm: −2.83 (s, 2H, −NH), 2.62 (s, 9H, $-CH_3$), 7.50 (m, 6H, phenyl H), 7.80 (m, 2H, phenyl H), 8.0 (m, 6H, phenyl H), 8.09 (m, 1H, phenyl H), 8.40 (m, 1H, phenyl H), 8.60 (m, 2H, pyrrole H), 8.80 (m, 6H, pyrrole H).

*5-(4-Carboxyphenyl)-10,15,20-tris(4-monomethyl triethyl ether phenoxy)porphyrin (**2p**)*. Yield: 11%. ^{1}H NMR ($CDCl_3$:400 MHz) δ ppm: −2.83 (s, 2H, -NH), 3.2 (s, 9H, $-CH_3$), 3.45 (m, 6H, $-CH_2$), 3.55 (m, 6H, $-CH_2$), 3.59 (m, 6H, $-CH_2$), 3.65 (m, 6H, $-CH_2$), 3.70 (m, 6H, $-CH_2$), 3.80 (m, 6H, CH_2), 7.20 (dd, 6H, phenyl H), 8.05 (dd, 6H, phenyl H), 8.2 (d, 2H, phenyl H), 8.35 (d, 2H, phenyl H), 8.70 (m, 2H, pyrrole H), 8.80 (m, 2H, pyrrole H).

*5-(3-Carboxyphenyl)-10,15,20-tris(4-monomethyl triethyl ether phenoxy)porphyrin (**2m**).* Yield: 10%. ^{1}H NMR ($CDCl_3$:400 MHz), δ ppm: −2.86 (s, 2H, −NH), 3.35 (s, 9H, $-CH_3$), 3.55 (m, 6H, $-CH_2$), 3.62 (m, 6H, $-CH_2$), 3.70 (m, 6H, $-CH_2$), 3.80 (m, 6H, $-CH_2$), 3.95 (m, 6H, $-CH_2$), 4.35 (m, 6H, CH_2) 7.20 (d, 6H, phenyl H), 7.79 (t, 1H, phenyl H), 7.90 (d, 1H, phenyl H), 8.05 (d, 6H, phenyl H), 8.32 (d, 1H, phenyl H), 8.40 (d, 1H, phenyl H), 8.75 (m, 2H, pyrrole H), 8.81 (m, pyrrole H).

*5-(3-Carboxyphenyl)-10,15,20-tris(4-propylphenyl)porphyrin (**3m**).* Yield: 14%. ^{1}H NMR ($CDCl_3$:400 MHz), δ ppm: −2.85 (s, 2H, −NH), 1.10 (m, 9H, $-CH_3$), 1.60 (m, 6H, $-CH_2$), 1.95 (m, 6H, $-6H_2$), 7.50 (d, 6H, phenyl H), 7.77 (t, 1H, phenyl H), 7.90 (d, 1H, phenyl H), 8.05 (d, 6H, phenyl H), 8.35 (d, 1H, phenyl H), 8.42 (d, 1H, phenyl H), 8.75 (m, 2H, pyrrole H), 8.85 (m, 6H, pyrrole H).

Synthesis of Zinc Porphyrins.[110] In a typical experiment, free-base porphyrin (90 mg) and zinc acetate (1:5 mol ratio) were refluxed in chloroform and methanol (1:1 ratio, 10 mL each) until free-base porphyrin was completely metalated; this was checked by the UV−vis spectrum, which showed disappearance of the 515 nm band. After evaporation of solvent, the crude compound was purified over silica gel column, and the desired compound was eluted by chloroform:methanol (95:5 v/v).

*[5-(4-Carboxyphenyl)-10,15,20-tris(tolyl)porphyrinato]zinc(II) (**1p-Zn**).* Yield, 85%. ^{1}H NMR ($CDCl_3$: 400 MHz), δ ppm: 2.70 (s, 9H, $-CH_3$), 7.60 (d, 6H, phenyl H), 8.15 (dd, 6H, phenyl H), 8.25 (d, 2H, phenyl H), 8.45 (d, 2H, phenyl H), 8.85 (d, 2H, pyrrole), 8.95 (m, 6H, pyrrole H).

*[5-(3-Carboxyphenyl)-10,15,20-tris(tolyl)porphyrinato]zinc(II) (**1m-Zn**).* Yield: 87%. ^{1}H NMR ($CDCl_3$:400 MHz), δ ppm: 2.60 (s, 9H, $-3CH_3$), 7.45 (d, 6H, phenyl H), 7.78 (m, 2H, phenyl H), 8.01 (d, 6H, phenyl H), 8.30 (d, 1H, phenyl H), 8.43 (d, 1H, phenyl H), 8.70 (m, 2H, pyrrole H), 8.81 (m, 6H, pyrrole H).

*[5-(2-Carboxyphenyl)-10,15,20-tris(tolyl)porphyrinato]zinc(II) (**1o-Zn**).* Yield: 80%. ^{1}H NMR ($CDCl_3$:400 MHz) δ ppm: 2.60 (s, 9H, $-CH_3$), 7.42 (m, 6H, phenyl H), 7.79 (m, 2H, phenyl H), 8.0 (m, 6H, phenyl H), 8.10 (m, 1H, phenyl H), 8.35 (m, 1H, phenyl H), 8.60 (m, 2H, pyrrole H), 8.79 (m, 6H, pyrrole H).

*[5-(4-Carboxyphenyl)-10,15,20-tris(4-phenyl monomethyl ethyl ether)porphyrinato] Zinc(II) (**2p-Zn**).* Yield: 78%. ^{1}H NMR ($CDCl_3$:400 MHz) δ ppm: 3.35 (s, 9H, $-CH_3$), 3.49 (m, 6H, $-CH_2$), 3.55 (m, 6H, $-CH_2$), 3.62 (m, 6H, $-CH_2$), 3.70 (m, 6H, $-CH_2$), 4.10 (m, 6H, $-CH_2$), 6.85 (dd, 6H, phenyl H), 7.92 (dd, 6H, phenyl H), 8.21 (m, 2H, phenyl H), 8.38 (m, 2H, phenyl H), 8.75 (m, 2H, pyrrole H), 8.82 (m, 6H, pyrrole H).

*[5-(4-Carboxyphenyl)-10,15,20-tris(4-propylphenyl)-porphyrinato]zinc(II) (**3p-Zn**).* Yield: 85%. ^{1}H NMR ($CDCl_3$:400 MHz), δ ppm: 1.20 (m, 9H, $-CH_3$), 1.65 (m, 6H, $-CH_2$), 1.95 (m, 6H, $-CH_2$),), 7.60 (d, 6H, phenyl H), 8.15 (dd, 6H, phenyl H), 8.35 (d, 2H, phenyl H), 8.40 (d, 2H, phenyl H), 8.85 (d, 2H, pyrrole), 8.95 (m, 6H, pyrrole H).

*[5-(3-Carboxyphenyl)-10,15,20-tris(4-propylphenyl)-porphyrinato]zinc(II) (**3m-Zn**).* Yield: 77%. ^{1}H NMR ($CDCl_3$:400 MHz), δ ppm: 0.95 (m, 9H, $-CH_3$), 1.30 (m, 6H, $-CH_3$), 1.95 (m, 6H, $-CH_2$), 7.45 (d, 6H, phenyl H), 7.78 (m, 2H, phenyl H), 8.05 (d, 6H, phenyl H), 8.38 (m, 2H), 8.70 (m, 2H, pyrrole H), 8.81 (m, 6H, pyrrole H).

*[5-(3-Carboxyphenyl)-10,15,20-tris(4-phenyl monomethyl ethyl ether)porphyrinato] zinc(II) (**2m-Zn**).* Yield: 76%. ^{1}H NMR ($CDCl_3$:400 MHz), δ ppm: 3.27 (s, 9H, $-CH_3$), 3.50 (m, 12H, $-CH_2$), 3.57 (m, 6H, $-CH_2$), 3.61 (m, 6H, $-CH_2$), 3.72 (m, 6H, $-CH_2$), 4.25 (m, 6H, $-CH_2$), 7.12 (d, 6H, phenyl H), 7.70 (t, 1H, phenyl H), 7.85 (d, 1H, phenyl H), 7.95 (d, 6H, phenyl H), 8.30 (m, 2H, phenyl H), 8.68 (m, 2H, pyrrole H), 8.79 (m, 6H, pyrrole H).

Spectral Measurements. The UV−visible measurements were collected either using a Jasco V-670 spectrophotometer or a Shimadzu model 2550 double monochromator UV−visible spectrophotometer. The steady state fluorescence spectra were measured using a Horiba Jobin Yvon Nanolog UV−visible−NIR spectrofluorometer equipped with a PMT (for UV−visible) and InGaAs (for NIR) detectors. The ^{1}H NMR studies were carried out on a Bruker 400 MHz spectrometer. Tetramethylsilane (TMS) was used as an internal standard. Differential pulse voltammograms were recorded on an EG&G 263A potentiostat/galvanostat using a three electrode system. A platinum button electrode was used as the working electrode, while a platinum wire served as the counter electrode and an Ag/AgCl electrode was used as the reference electrode. Ferrocene/ferrocenium redox couple was used as an internal standard. All the solutions were purged prior to electrochemical and spectral measurements with nitrogen gas.

Photoelectrochemical Measurements. Photoelectrochemical measurements were performed using the Grätzel-type two-electrode system using FTO (∼10−12 μm, tec7 grade from Pilkington) glass coated with thin film TiO_2 as the working electrode and Pt-ized FTO as the counter electrode. The thin film TiO_2 was prepared via the "Doctor blade" technique as reported earlier.[80] A mediator solution containing 0.1 M LiI, 0.05 M I_2, and 0.5 M 4-*t*-butylpyridine in acetonitrile was injected between the electrodes.

The photocurrent-photovoltage characteristics were collected using a Keithley Instruments Inc. (Cleveland, OH) model 2400 current/voltage source meter under illumination from a simulated light source using a Model 9600 of 150-W Solar Simulator of Newport Corp. (Irvine, CA) and filtered using an AM 1.5 filter. Incident photon-to-current efficiency (IPCE) measurements were performed under ∼4 mW cm^2 monochromatic light illumination conditions using a setup comprised of a 150 W Xe lamp with a Cornerstone 260 monochromator (Newport Corp., Irvine, CA).

Electrochemical Impedance Measurements. Electrochemical impedance measurements were performed using EG&G PARSTAT 2273 potentiostat/galvanostat. Impedance data were recorded under forward bias condition from 100 kHz to 50 mHz with an AC amplitude of 10 mV. Data were recorded under dark and A.M 1.5 illumination conditions applying corresponding open circuit potential (V_{oc}). The data were analyzed using ZSimpwin software from Princeton Applied Research. Solution resistance (R_s), charge transfer resistance (R_{ct}), and capacitance due to constant phase element (Q) were deduced from the fitted data. CPE was considered as capacitance component of the double-layer electrode interface due to roughness of the electrode.

Femtosecond Transient Absorption Spectral Measurements. Femtosecond transient absorption spectroscopy experiments were performed using an Ultrafast Femtosecond Laser Source (Libra) by Coherent incorporating diode-pumped, mode locked Ti:Sapphire laser (Vitesse) and diode-pumped intra cavity doubled Nd:YLF laser (Evolution) to generate a compressed laser output of 1.45 W. For optical detection a Helios transient absorption spectrometer coupled with femtosecond harmonics generator both provided by Ultrafast Systems LLC was used. The source for the pump and probe pulses were derived from the fundamental output of Libra (Compressed output 1.45 W, pulse width 91 fs) at a repetition rate of 1 kHz. 95% of the fundamental output of the laser was introduced into harmonic generator which produces second and third harmonics of 400 and 267 nm besides the fundamental 800 nm for excitation, while the rest of the output was used for generation of white light continuum. In the present study, the second harmonic 400 nm excitation pump was used in all the experiments. Kinetic traces at appropriate wavelengths were assembled from the time-resolved spectral data. All measurements were conducted at 298 K.

Preparation of Electrodes for Photoelectrochemical and Transient Studies. Electrodes were prepared by cleaning FTO by sonicating individually in solutions of 0.1 M HCl, acetone, and isopropanol. Next, the FTO was allowed to soak in 20 mM solution of $TiCl_4$ at 70 °C for 30 min. Then, a layer of 20 nm anatase TiO_2 (18 NRT, Dyesol) was applied on the surface of the FTO using the doctor blade technique and allowed to dry in air for 20 min. The FTO/TiO_2 was then annealed in a heat cycle of 130, 230, 330, 390, 440, and 515 °C for 10 min each. After cooling, a second layer of 20 nm anatase TiO_2 was applied and annealed in a similar fashion. Next, the electrodes were allowed to soak in a fresh $TiCl_4$ solution for an additional 30 min at 70 °C. Then the films were annealed at 440 °C for 30 min and then cooled at 130 °C before immersing in 0.2 mM sensitizer solution for 4 h.

■ ASSOCIATED CONTENT

Supporting Information

Spectra of oxidized porphyrins, **1p-Zn** and **1o-Zn** in methanol, and femtosecond transient spectra of **1o-Zn** in *o*-dichlorobenzene and FTO/TiO_2/**1m-Zn** electrode. This material is available free of charge via the Internet at http://pubs.acs.org/.

■ AUTHOR INFORMATION

Corresponding Author

*E-mail: Francis.DSouza@UNT.edu.

Notes

The authors declare no competing financial interest.

■ ACKNOWLEDGMENTS

This work was supported by the National Science Foundation (Grant 1110942 to F.D). L.R.S. is thankful to NSF-REU (CHE-1004878) for a summer fellowship.

■ REFERENCES

(1) O'Regan, B.; Grätzel, M. *Nature* **1991**, *353*, 737.
(2) Grätzel, M. *Nature* **2001**, *414*, 338.
(3) Nazeeruddin, M. K.; Pechy, P.; Renouard, T.; Zakeeruddin, S. M.; Humphry-Baker, R.; Comte, P.; Liska, P.; Cevey, L.; Costa, E.; Shklover, V.; Spiccia, L.; Deacon, G. B.; Bignozzi, C. A.; Grätzel, M. *J. Am. Chem. Soc.* **2001**, *123*, 1613.
(4) Nazeeruddin, M. K.; De Angelis, F.; Fantacci, S.; Selloni, A.; Viscardi, G.; Liska, P.; Ito, S.; Bessho, T.; Grätzel, M. *J. Am. Chem. Soc.* **2005**, *127*, 16835.
(5) Chiba, Y.; Islam, A.; Watanabe, Y.; Komiya, R.; Koide, N.; Han, L. Y. *Jpn. J. Appl. Phys.* **2006**, *45*, L638.
(6) Nazeeruddin, M. K.; Bessho, T.; Cevey, L.; Ito, S.; Klein, C.; De Angelis, F.; Fantacci, S.; Comte, P.; Liska, P.; Imai, H.; Grätzel, M. *J. Photochem. Photobiol. A* **2007**, *185*, 331.
(7) Gao, F.; Wang, Y.; Shi, D.; Zhang, J.; Wang, M. K.; Jing, X. Y.; Humphry-Baker, R.; Wang, P.; Zakeeruddin, S. M.; Grätzel, M. *J. Am. Chem. Soc.* **2008**, *130*, 10720.
(8) Chen, C. Y.; Wang, M. K.; Li, J. Y.; Pootrakulchote, N.; Alibabaei, L.; Ngocle, C. H.; Decoppet, J. D.; Tsai, J. H.; Gratzel, C.; Wu, C. G.; Zakeeruddin, S. M.; Grätzel, M. *ACS Nano* **2009**, *3*, 3103.
(9) Hagfeldt, A.; Boschloo, G.; Sun, L.; Kloo, L.; Pettersson, H. *Chem. Rev.* **2010**, *110*, 6595.
(10) Cao, Y. M.; Bai, Y.; Yu, Q. J.; Cheng, Y. M.; Liu, S.; Shi, D.; Gao, F. F.; Wang, P. *J. Phys. Chem. C* **2009**, *113*, 6290.
(11) Han, L. Y.; Islam, A.; Chen, H.; Malapaka, C.; Chiranjeevi, B.; Zhang, S. F.; Yang, X. D.; Yanagida, M. *Energy Environ. Sci.* **2012**, *5*, 6057.
(12) Moser, J. E.; Bonnote, P.; Grätzel, M. *Coord. Chem. Rev.* **1998**, *171*, 245.
(13) Robertson, N. *Angew. Chem., Int. Ed.* **2006**, *45*, 2338.
(14) Pelet, S.; Grätzel, M.; Moser, J. E. *J. Phys. Chem. B* **2003**, *107*, 3215.
(15) Haque, S. A.; Tachibana, Y.; Willis, R. L.; Moser, J. E.; Grätzel, M.; Klug, D. R.; Durrant, J. R. *J. Phys. Chem. B* **2000**, *104*, 538.
(16) Chen, C.; Wang, M.; Wang, K. *J. Phys. Chem. C* **2009**, *113*, 1624.
(17) Myllyperkio, P.; Manzoni, C.; Polli, D.; Cerullo, G.; Korppi-Tommola, J. *J. Phys. Chem. C* **2009**, *113*, 13985.
(18) Wiberg, J.; Marinado, T.; Hagberg, D. P.; Sun, L. C.; Hagfeldt, A.; Albinsson, B. *J. Phys. Chem. C* **2009**, *113*, 3881.
(19) Ravirajan, P.; Peiró, A. M.; Nazeeruddin, M. K.; Grätzel, M.; Bradley, D. D. C.; Durrant, J. R.; Nelson, J. *J. Phys. Chem. B* **2006**, *110*, 7635.
(20) Anderson, S.; Constable, E. C.; Dareedwards, M. P.; Goodenough, J. B.; Hamnett, A.; Seddon, K. R.; Wright, R. D. *Nature* **1979**, *280*, 571.
(21) Tachibana, Y.; Moser, J. E.; Grätzel, M.; Klug, D. R.; Durrant, J. R. *J. Phys. Chem.* **1996**, *100*, 20056.
(22) Hannappel, T.; Burfeindt, B.; Storck, W.; Willig, F. *J. Phys. Chem. B* **1997**, *101*, 6799.
(23) Moser, J. E.; Noukakis, D.; Bach, U.; Tachibana, Y.; Klug, D. R.; Durrant, J. R.; Humphry-Baker, R.; Grätzel, M. *J. Phys. Chem. B* **1998**, *102*, 3649.
(24) Ellingson, R. J.; Asbury, J. B.; Ferrere, S.; Ghosh, H. N.; Sprague, J. R.; Lian, T. Q.; Nozik, A. J. *J. Phys. Chem. B* **1998**, *102*, 6455.
(25) Asbury, J. B.; Ellingson, R. J.; Ghosh, H. N.; Ferrere, S.; Nozik, A. J.; Lian, T. Q. *J. Phys. Chem. B* **1999**, *103*, 3110.
(26) Durrant, J. R.; Tachibana, Y.; Mercer, I.; Moser, J. E.; Grätzel, M.; Klug, D. R. Z. *Phys. Chem* **1999**, *212*, 93.
(27) Tachibana, Y.; Haque, S. A.; Mercer, I. P.; Durrant, J. R.; Klug, D. R. *J. Phys. Chem. B* **2000**, *104*, 1198.
(28) Haque, S. A.; Handa, S.; Peter, K.; Palomares, E.; Thelakkat, M.; Durrant, J. R. *Angew. Chem., Int. Ed.* **2005**, *44*, 5740.
(29) Nelson, J.; Haque, S. A.; Klug, D. R.; Durrant, J. R. *Phys. Rev. B* **2001**, *63*, 205321.
(30) Heimer, T. A.; Heilweil, E. J.; Bignozzi, C. A.; Meyer, G. J. *J. Phys. Chem. A* **2000**, *104*, 4256.
(31) Kallioinen, J.; Lehtovuori, V.; Myllyperkio, P.; Korppi-Tommola, J. *Chem. Phys. Lett.* **2001**, *340*, 217.
(32) Benko, G.; Kallioinen, J.; Korppi-Tommola, J. E. I.; Yartsev, A. P.; Sundström, V. *J. Am. Chem. Soc.* **2002**, *124*, 489.
(33) Kallioinen, J.; Benko, G.; Sundström, V.; Korppi-Tommola, J. E. I.; Yartsev, A. P. *J. Phys. Chem. B* **2002**, *106*, 4396.
(34) Anderson, N. A.; Lian, T. *Coord. Chem. Rev.* **2004**, *248*, 1231.
(35) Schwarzburg, K.; Ernstorfer, R.; Felber, S.; Willig, F. *Coord. Chem. Rev.* **2004**, *248*, 1259.
(36) Barzykin, A. V.; Tachiya, M. *J. Phys. Chem. B* **2002**, *106*, 4356.
(37) Katoh, R.; Furube, A.; Barzykin, A. V.; Arakawa, H.; Tachiya, M. *Coord. Chem. Rev.* **2004**, *248*, 1195.
(38) Barzykin, A. V.; Tachiya, M. *J. Phys. Chem. B* **2004**, *108*, 8385.
(39) Pan, J.; Benko, G.; Xu, Y. H.; Pascher, T.; Sun, L. C.; Sundström, V.; Polivka, T. *J. Am. Chem. Soc.* **2002**, *124*, 13949.
(40) Wang, D.; Mendelsohn, R.; Galoppini, E.; Hoertz, P. G.; Carlisle, R. A.; Meyer, G. J. *J. Phys. Chem. B* **2004**, *108*, 16642.
(41) Kilsa, K.; Mayo, E. I.; Kuciauskas, D.; Villahermosa, R.; Lewis, N. S.; Winkler, J. R.; Gray, H. B. *J. Phys. Chem. A* **2003**, *107*, 3379.
(42) Tian, H. N.; Yang, X. C.; Cong, J. Y.; Chen, R. K.; Liu, J.; Hao, Y.; Hagfeldt, A.; Sun, L. *C. Chem. Commun.* **2009**, 6288.
(43) Wang, Z. S.; Koumura, N.; Cui, Y.; Miyashita, M.; Mori, S.; Hara, K. *Chem. Mater.* **2009**, *21*, 2810.
(44) Qin, H.; Wenger, S.; Xu, M.; Gao, F.; Jing, X.; Wang, P.; Zakeeruddin, S. M.; Grätzel, M. *J. Am. Chem. Soc.* **2008**, *130*, 9202.
(45) Zhou, G.; Pschirer, N.; Schoneboom, J. C.; Eickemeyer, F.; Baumgarten, M.; Mullen, K. *Chem. Mater.* **2008**, *20*, 1808.
(46) Xu, W.; Peng, B.; Chen, J.; Liang, M.; Cai, F. *J. Phys. Chem. C* **2008**, *112*, 874.
(47) Li, G.; Jiang, K.-J.; Li, Y.-F.; Li, S.-L.; Yang, L.-M. *J. Phys. Chem. C* **2008**, *112*, 11591.
(48) Ning, Z. J.; Zhang, Q.; Wu, W. J.; Pei, H. C.; Liu, B.; Tian, H. *J. Org. Chem.* **2008**, *73*, 3791.
(49) Horiuchi, T.; Miura, H.; Sumioka, K.; Uchida, S. *J. Am. Chem. Soc.* **2004**, *126*, 12218.
(50) Zhang, X. H.; Wang, Z. S.; Cui, Y.; Koumura, N.; Furube, A.; Hara, K. *J. Phys. Chem. C* **2009**, *113*, 13409.
(51) Hara, K.; Sayama, K.; Ohga, Y.; Shinpo, A.; Suga, S.; Arakawa, H. A. *Chem. Commun.* **2001**, 569.
(52) Wang, Z. S.; Cui, Y.; Dan-Oh, Y.; Kasada, C.; Shinpo, A.; Hara, K. *J. Phys. Chem. C* **2007**, *111*, 7224.
(53) Wang, Z. S.; Cui, Y.; Dan-Oh, Y.; Kasada, C.; Shinpo, A.; Hara, K. *J. Phys. Chem. C* **2008**, *112*, 17011.
(54) Horiuchi, T.; Miura, H.; Uchida, S. *Chem. Commun.* **2003**, 3036.
(55) Hara, K.; Kurashige, M.; Ito, S.; Shinpo, A.; Suga, S.; Sayama, K.; Arakawa, H. *Chem. Commun.* **2003**, 252.
(56) Kitamura, T.; Ikeda, M.; Shigaki, K.; Inoue, T.; Anderson, N. A.; Ai, X.; Lian, T. Q.; Yanagida, S. *Chem. Mater.* **2004**, *16*, 1806.

(57) Hwang, S.; Lee, J. H.; Park, C.; Lee, H.; Kim, C.; Park, C.; Lee, M.-H.; Lee, W.; Park, J.; Kim, K.; Park, N.-G.; Kim, C. A. *Chem. Commun.* **2007**, 4887.
(58) Kim, C.; Choi, H.; Kim, S.; Baik, C.; Song, K.; Kang, M. S.; Kang, S. O.; Ko, J. *J. Org. Chem.* **2008**, *73*, 7072.
(59) Im, H.; Kim, S.; Park, C.; Jang, S. H.; Kim, C. J.; Kim, K.; Park, N. G.; Kim. *C. Chem. Commun.* **2010**, *46*, 1335.
(60) Tan, S. X.; Zhai, J.; Fang, H. J.; Jiu, T. G.; Ge, J.; Li, Y. L.; Jiang, L.; Zhu, D. B. *Chem.—Eur. J.* **2005**, *11*, 6272.
(61) Liu, W. H.; Wu, I. C.; Lai, C. H.; Chou, P. T.; Li, Y. T.; Chen, C. L.; Hsu, Y. Y.; Chi, Y. *Chem. Commun.* **2008**, 5152.
(62) Wang, Z. S.; Koumura, N.; Cui, Y.; Takahashi, M.; Sekiguchi, H.; Mori, A.; Kubo, T.; Furube, A.; Hara, K. *Chem. Mater.* **2008**, *20*, 3993.
(63) Wu, W. J.; Hua, J. L.; Jin, Y. H.; Zhan, W. H.; Tian, H. *Photochem. Photobiol. Sci.* **2008**, *7*, 63.
(64) Yum, J. H.; Walter, P.; Huber, S.; Rentsch, D.; Geiger, T.; Nuesch, F.; De Angelis, F.; Grätzel, M.; Nazeeruddin, M. K. *J. Am. Chem. Soc.* **2007**, *129*, 10320.
(65) Reddy, P. Y.; Giribabu, L.; Lyness, C.; Snaith, H. J.; Vijaykumar, C.; Chandrasekharan, M.; Lakshmikantam, M.; Yum, J. H.; Kalyanasundaram, K.; Grätzel, M.; Nazeeruddin, M. K. *Angew. Chem., Int. Ed.* **2007**, *46*, 373.
(66) Cid, J. J.; Yum, J. H.; Jang, S. R.; Nazeeruddin, M. K.; Ferrero, E. M.; Palomares, E.; Ko, J.; Grätzel, M.; Torres, T. *Angew. Chem., Int. Ed.* **2007**, *46*, 8358.
(67) Martinez-Diaz, M. V.; de la Torre, G.; Torres, T. *Chem. Commun.* **2010**, *46*, 7090.
(68) Mori, S.; Nagata, M.; Nakahata, Y.; Yasuta, K.; Goto, R.; Kimura, M.; Taya, M. *J. Am. Chem. Soc.* **2010**, *132*, 4054.
(69) Ragoussi, M. E.; Cid, J. J.; Yum, J. H.; de la Torre, G.; Di Censo, D.; Grätzel, M.; Nazeeruddin, M. K.; Torres, T. *Angew. Chem., Int. Ed.* **2012**, *51*, 4375.
(70) Ferrere, S.; Zaban, A.; Gregg, B. A. *J. Phys. Chem. B* **1997**, *101*, 4490.
(71) Shibano, Y.; Umeyama, T.; Matano, Y.; Imahori, H. *Org. Lett.* **2007**, *9*, 1971.
(72) Li, C.; Yum, J. H.; Moon, S. J.; Herrmann, A.; Eickemeyer, F.; Pschirer, N. G.; Erk, P.; Schoeboom, J.; Mullen, K.; Grätzel, M.; Nazeeruddin, M. K. *ChemSusChem* **2008**, *1*, 615.
(73) Mathew, S.; Imahori, H.; Tunable. *J. Mater. Chem.* **2011**, *21*, 7166.
(74) Zhang, G. L.; Bala, H.; Cheng, Y. M.; Shi, D.; Lv, X. J.; Yu, Q. J.; Wang, P. *Chem. Commun.* **2009**, 2198.
(75) Zeng, W. D.; Cao, Y. M.; Bai, Y.; Wang, Y. H.; Shi, Y. S.; Zhang, M.; Wang, F. F.; Pan, C. Y.; Wang, P. *Chem. Mater.* **2010**, *22*, 1915.
(76) Tian, H.; Yang, X.; Chen, R.; Pan, Y.; Li, L.; Hagfeldt, A.; Sun, L. *Chem. Commun.* **2007**, 3741.
(77) Cao, D.; Peng, J.; Hong, Y.; Fang, X.; Wang, L.; Meier, H. *Org. Lett.* **2011**, *13*, 1610.
(78) Xie, Z.; Midya, A.; Loh, K. P.; Adams, S.; Blackwood, D. J.; Wang, J.; Zhang, X.; Chen, Z. *Prog. Photovoltaics* **2010**, *18*, 573.
(79) Wu, W.; Yang, J.; Hua, J.; Tang, J.; Zhang, L.; Long, Y.; Tian, H. *J. Mater. Chem.* **2010**, *20*, 1772.
(80) Hart, A. S.; KC, C. B.; Subbaiyan, N. K.; Karr, P. A.; D'Souza, F. *ACS Appl. Mater. Inter.* **2012**, *4*, 5813.
(81) Sargent, E. H. *Nat. Photonics* **2012**, *6*, 133.
(82) Bang, J. H.; Kamat, P. V. *ACS Nano* **2009**, *3*, 1467.
(83) Tang, J.; Wang, X.; Brzozowski, L.; Barkhouse, D.; Aaron, R.; Debnath, R.; Levina, L.; Sargent, E. H. *Adv. Mater.* **2010**, *22*, 1398.
(84) Wang, Q.; Campbell, W. M.; Bonfantani, E. E.; Jolley, K. W.; Officer, D. L.; Walsh, P. J.; Gordon, K.; Humphry-Baker, R.; Nazeeruddin, M. K.; Grätzel, M. *J. Phys. Chem. B* **2005**, *109*, 15397.
(85) Campbell, W. M.; Jolley, K. W.; Wagner, P.; Wagner, K.; Walsh, P. J.; Gordon, K. C.; Schmidt-Mende, L.; Nazeeruddin, M. K.; Wang, Q.; Grätzel, M.; Officer, D. L. *J. Phys. Chem. C* **2007**, *111*, 11760.
(86) Lee, C. Y.; She, C. X.; Jeong, N. C.; Hupp, J. T. *Chem. Commun.* **2010**, *46*, 6090.
(87) Imahori, H.; Umeyama, T.; Ito, S. *Acc. Chem. Res.* **2009**, *42*, 1809.
(88) Walter, M. G.; Rudine, A. B.; Wamser, C. C. *J. Porphyrins Phthalocyanines* **2010**, *14*, 759.
(89) Imahori, H.; Matsubara, Y.; Iijima, H.; Umeyama, T.; Matano, Y.; Ito, S.; Niemi, M.; Tkachenko, N. V.; Lemmetyinen, H. *J. Phys. Chem. C* **2010**, *114*, 10656.
(90) Kira, A.; Matsubara, Y.; Iijima, H.; Umeyama, T.; Matano, Y.; Ito, S.; Niemi, M.; Tkachenko, N. V.; Lemmetyinen, H.; Imahori, H. *J. Phys. Chem. C* **2010**, *114*, 11293.
(91) Mathew, S.; Iijima, H.; Toude, Y.; Umeyama, T.; Matano, Y.; Ito, S.; Tkachenko, N. V.; Lemmetyinen, H.; Imahori, H. *J. Phys. Chem. C* **2011**, *115*, 14415.
(92) Imahori, H.; Umeyama, T.; Kurotobi, K.; Takano, Y. *Chem. Commun.* **2012**, *48*, 4032.
(93) Ye, S.; Kathiravan, A.; Hayashi, H.; Tong, Y.; Infahsaeng, Y.; Chabera, P.; Pascher, T.; Yartsev, A. P.; Isoka, S.; Imahori, H.; Sundström, V. *J. Phys. Chem.* **2013**, *117*, 6066.
(94) Subbaiyan, N. K.; Wijesinghe, C. A.; D'Souza, F. *J. Am. Chem. Soc.* **2009**, *131*, 14646.
(95) Hasobe, T. *Phys. Chem. Chem. Phys.* **2010**, *12*, 44.
(96) Ishida, M.; Park, S. W.; Hwang, D.; Koo, Y. B.; Sessler, J. L.; Kim, D. Y.; Kim, D. *J. Phys. Chem. C* **2011**, *115*, 19343.
(97) Wang, F.; Subbaiyan, N. K.; Wang, Q.; Rochford, C.; Xu, G.; Lu, R.; Elliot, A.; D'Souza, F.; Hut, R.; Wu, J. *ACS Appl. Mater. Interfaces* **2012**, *4*, 1565.
(98) KC, C. B.; Stranius, K.; D'Souza, P.; Subbaiyan, N. K.; Lemmetyinen, H.; Tkachenko, N. V.; D'Souza, F. *J. Phys. Chem. C.* **2013**, *117*, 763.
(99) Subbaiyan, N. K.; Hill, J. P.; Ariga, K.; Fukuzumi, S.; D'Souza, F. *Chem. Commun.* **2011**, *47*, 6003.
(100) Cherian, S.; Wamser, C. C. *J. Phys. Chem. B* **2000**, *104*, 3624.
(101) Rochford, J.; Chu, D.; Hagfeldt, A.; Galoppini, E. *J. Am. Chem. Soc.* **2007**, *129*, 4655.
(102) Rangan, S.; Katallinic, S.; Thorpe, R.; Bartynski, R. A.; Rochford, J.; Galoppini, E. *J. Phys.Chem. C* **2010**, *114*, 1139.
(103) Rochford, J.; Galoppini, E. *Langmuir* **2008**, *24*, 5366.
(104) Ma, T. L.; Inoue, K.; Noma, H.; Yao, K.; Abe, E. *J. Photochem. Photobiol. A: Chem.* **2002**, *152*, 207.
(105) Bessho, T.; Zakeeruddin, S. M.; Yeh, C. Y.; Diau, E. W. G.; Grätzel, M. *Angew. Chem., Int. Ed.* **2010**, *49*, 6646.
(106) Wang, C. L.; Chang, Y. C.; Lan, C. M.; Lo, C. F.; Diau, E. W. G.; Lin, C. Y. *Energy Environ. Sci.* **2011**, *4*, 1788.
(107) Chang, Y. C.; Wang, C. L.; Pan, T. Y.; Hong, S. H.; Lan, C. M.; Kuo, H. H.; Lo, C. F.; Hsu, H. Y.; Lin, C. Y.; Diau, E. W. *Chem. Commun.* **2011**, *47*, 8910.
(108) Yella, A.; Lee, H. W.; Tsao, H. N.; Yi, C. Y.; Chandiran, A. K.; Nazeeruddin, M. K.; Diau, E. W. G.; Yeh, C. Y.; Zakeeruddin, S. M.; Grätzel, M. *Science* **2011**, *334*, 629.
(109) Kim, J. B.; Adler, A. D.; Long, F. R. In *The Porphyrins*; Dolphin, D., Ed.; Academic Press: New York, 1978; Vol. *IA*, pp 85−100.
(110) Smith, K. M. *Porphyrins and Metalloporphyrins*; Elsevier: Amsterdam, 1972; pp 798.
(111) Gouterman, M. *J. Mol. Spectrosc.* **1961**, *6*, 138−163.
(112) McHugh, A. J.; Gouterman, M.; Weiss, C., Jr. *Theor. Chim. Acta* **1972**, *24*, 346−70.
(113) Kadish, K. M. *Prog. Inorg. Chem.* **1986**, *34*, 435.
(114) *Dye-Sensitized Solar Cells*; Kalyanasundaram, K., Ed.; EPFL Press: Lausanne, Switzerland, 2010.
(115) Hasobe, T.; Saito, K.; Kamat, P. V.; Troiani, V.; Qui, H.; Solladie, N.; Kim, K. S.; Park, J. K.; Kim, D.; D'Souza, F.; Fukuzumi, S. *J. Mater. Chem.* **2007**, *17*, 4160.
(116) Bisquert, J.; Fabregat-Santiago, F. In *Dye-Sensitized Solar Cells*; Kalyanasundaram, K., Ed.; EPFL Press: Lausanne, Switzerland, 2010; Chapter 12, pp 457−554.
(117) Subbaiyan, N. K.; Maligaspe, E.; D'Souza, F. *ACS Appl. Mater. Interfaces* **2011**, *3*, 2368.
(118) Chang, C.-W.; Luo, L.; Chou, C.-K.; Lo, C.-F.; Lin, C.-Y.; Hung, C.-S.; Lee, Y.-P.; Diau, E. W. G. *J. Phys. Chem. C.* **2009**, *113*, 11524.
(119) Imahori, H.; Kang, S.; Hayashi, H.; Haruta, M.; Kurata, H.; Isoda, S.; Canton, S.; Infahsaeng, Y.; Kathiravan, A.; Pascher, T.; Chábera, P.; Yartsev, A.; Sundström, V. *J. Phys. Chem. A* **2011**, *115*, 3679.